Carbohydrate Polymers 118 (2015) 242–249

Contents lists available at ScienceDirect

Carbohydrate Polymers

journal homepage: www.elsevier.com/locate/carbpol

A novel metal coordination enabled in carboxylated alginic acid for effective fluoride removal

Kalimuthu Pandi, Natrayasamy Viswanathan*

Department of Chemistry, Anna University, University College of Engineering – Dindigul, Reddiyarchatram, Dindigul- 624 622, Tamilnadu, India

ARTICLE INFO

Article history:
Received 26 August 2014
Received in revised form 27 October 2014
Accepted 31 October 2014
Available online 7 November 2014

Keywords:
Alginic acid
Carboxylated alginic acid
Metal coordination
Fluoride
Sorption
Field application

ABSTRACT

This article enlightens the synthesis of carboxylated alginic acid (CAA) and metal ions coordinated CAA (M-CAA) for defluoridation studies in batch mode. The oxidation of alginic acid (AA) with $KMnO_4$ gives CAA and the metal coordination was enabled in CAA by using high valence metal ions viz., La^{3+} (La-CAA) and Zr^{4+} (Zr-CAA). The synthesized materials Zr-CAA, La-CAA and CAA possess the defluoridation capacities (DCs) of 4064, 3137 and 880 mgF^-/kg respectively. An enhanced DC was observed for metal-coordinated CAA (M-CAA) than CAA. The defluoridation experiments were carried with numerous influencing parameters like contact time, pH and competitor anions for optimization. The characterization of materials was carried out using FTIR, EDAX and SEM analysis. The sorption data was fitted with various isotherms and kinetic models. The values of thermodynamic parameters indicate the nature of fluoride removal is spontaneous and endothermic. At field conditions, M-CAA reduce the fluoride concentration below the tolerance limit.

1. Introduction

The fluoride enters into the drinking water either by the dissolution of fluoride bearing minerals and/or anthropogenic activities. The amount of fluoride in drinking water leads to beneficial and detrimental effects on health. At lower concentration, it helps to strengthen the teeth and repair the damage caused by early tooth decay before it becomes permanent, but exposed to higher levels (>1.5 mg/L as per WHO) leads to fluorosis (WHO, 2006). Researchers developed numerous conventional treatment techniques to remove the excess fluoride from the water bodies namely chemical precipitation (Lu & Liu, 2010), reverse osmosis (Ndiaye, Moulin, Dominguez, Millet, & Charbit, 2005), electro-coagulation (Vasudevan, Lakshmi, & Sozhan, 2009), nanofiltration (Tahaikt et al., 2007), ion exchange (Meenakshi & Viswanathan, 2007) and adsorption (Viswanathan & Meenakshi, 2010). In the last decade, adsorption is one of the most promising techniques for fluoride removal due to its ease of operation, uptake capacity, cost–effective and no sludge generation.

Biosorption is the one of the environmentally sound techniques which minimize the operation cost and make the adsorption technology more feasible and eco-friendly. In this scenario, scientists have paid increased attention on the development of bioadsorbents using chitin, chitosan, alginate, cellulose, etc., for the removal of toxic ions from the aqueous solution (Googerdchian, Moheb, & Emadi, 2012; Jayakumar et al., 2009; Pandi & Viswanathan, 2014; Sairam Sundaram, Viswanathan, & Meenakshi, 2009; Varma, Deshpande, & Kennedy, 2004; Viswanathan & Meenakshi, 2009a; Yu, Tong, Ge, & Zuo, 2013). Among them, alginic acid has been regarded as a fabulous biopolymer because of its unique characteristics such as biodegradability, biocompatibility and non-toxicity. In addition, the reactive carboxyl and hydroxyl functional groups are the attractive features of AA. The functionalization of adsorbent material will increase its selectivity toward a particular ion. In order to effectively utilize the hydroxyl groups in the alginic acid, an oxidation reaction was carried out using $KMnO_4$, which converts the hydroxyl groups of AA into carboxyl groups namely carboxylated alginic acid (Jeon, Park, & Yoo, 2002). Recently higher valence metal ions incorporated materials are focused to develop new adsorbents with good performance for the selective removal of fluoride (Paudyal et al., 2013; Viswanathan & Meenakshi, 2008, 2009b). Hence, the higher valence metal ions viz., La^{3+} and Zr^{4+} ions have been utilized for enabling metal coordination with CAA which helps to increase its strength and uptake capacity.

The ultimate aim of the present work is to develop low cost, eco-friendly, functionalized and metal coordinated biomaterials for fluoride removal. Based on the above aspiration, the authors have synthesized carboxylated alginic acid and metal coordinated carboxylated alginic acid for defluoridation studies. A comparative evaluation of CAA and M-CAA was also made. The sorption studies

* Corresponding author. Tel.: +91 451 2554066; fax: +91 451 2554066.
E-mail address: drnviswanathan@gmail.com (N. Viswanathan).

http://dx.doi.org/10.1016/j.carbpol.2014.10.068
0144-8617/

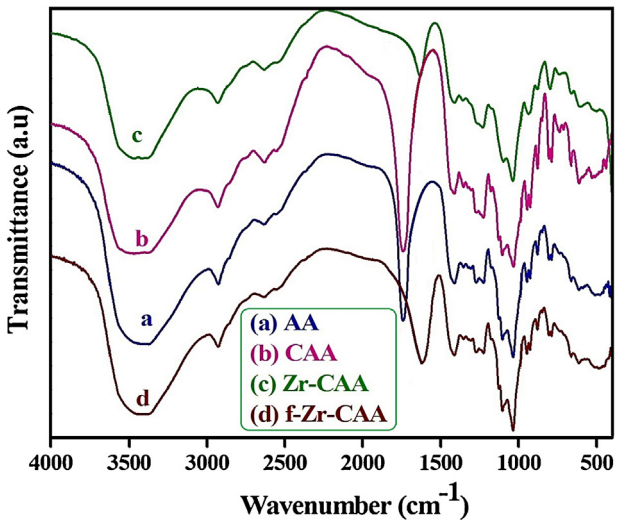

Fig. 1. FTIR spectra of (a) AA, (b) CAA, (c) Zr-CAA and (d) fluoride sorbed Zr-CAA (f-Zr-CAA).

were carried out to optimize various equilibrating conditions like contact time, pH, presence of competitor anions, different initial fluoride concentrations and temperature. Adsorption data have been fitted to various isotherms and kinetic models. The thermodynamic parameters viz., ΔG°, ΔH° and ΔS° have also been calculated and interpreted. The application of the biosorbents at field conditions was also tested by collecting the field fluoride water sample in a nearby fluoride widespread area.

2. Materials and methods

2.1. Materials

Alginic acid used in the work was purchased from Central Drug House (India). $KMnO_4$, $LaCl_3{\cdot}7H_2O$, $ZrOCl_2{\cdot}8H_2O$ and other chemicals used in the work were of analytical grade and used without further purification. Double distilled water was used to prepare the standard solutions.

2.2. Synthesis of CAA and M-CAA

The carboxylated alginic acid (CAA) was prepared as suggested by Jeon et al. (2002). Briefly, 10 g of alginic acid was added into the 10 mM of $KMnO_4$ solution and stirred for 30 min at 30 °C. Then the reacted mixture was separated by centrifugation and thoroughly washed with distilled water and then dried at 60 °C for 2 h in hot air oven. The synthesis of metal coordinated carboxylated alginic acid (M-CAA) as follows. About 0.1 mol of La(III) and Zr(IV) solution were prepared separately by dissolving appropriate amount of $LaCl_3{\cdot}7H_2O$ and $ZrOCl_2{\cdot}8H_2O$ in 100 mL of distilled water respectively. About 2 g of synthesized CAA was added into the respective metal ion solutions and the mixture was gently stirred for 24 h at room temperature. Finally the mixture was filtered and thoroughly washed with distilled water and then dried at 60 °C for 6 h in hot air oven. The dried sorbents was grinded to fine powder using ball mill (IKA, Germany) and then used for fluoride sorption studies.

2.3. Fluoride sorption experiments

The synthesized materials were utilized as sorbents for the removal of fluoride from the aqueous solution by the batch equilibration method in duplicate. Experiments were conducted by adding 0.1 g of dry sorbent into 50 mL of 10 mg/L sodium fluoride solution at room temperature. The influence of pH on fluoride sorption by the sorbents was studied by varying the pH of the solution in the range of 3–11 using 0.1 M HCl/NaOH solution. The mixture was shaken in an orbital shaker rotating with a speed of 200 rpm at room temperature. Samples were taken at prefixed time intervals for the analysis of fluoride concentrations in the solutions until sorption equilibrium was reached. Thermodynamic studies were carried out using waterbath shaker with different initial fluoride concentrations, viz., 8, 10, 12 and 14 mg/L in the temperature range of 303, 313 and 323 K. After equilibrating time, the samples were filtered and the final fluoride concentration was determined.

2.4. Analysis

The fluoride concentration was measured using Thermo Orion Benchtop multiparameter kit (VERSA STAR 92) with the fluoride ion selective electrode (Thermo Orion, USA). The pH measurements were made with the same instrument using pH electrode. All other water quality parameters were investigated using standard methods (APHA, 2005). The pH at zero point charge (pH_{zpc}) of the sorbent was determined by pH drift method (Lopez-Ramon, Stoeckli, Moreno-Castilla, & Carrasco-Marin, 1999).

2.5. Characterization techniques

Fourier transform infrared (FTIR) spectra of the materials were carried out using JASCO-460 plus spectrophotometer operated at 1 cm^{-1} resolution in 400–4000 cm^{-1} region using KBr pellets. The surface morphology of the sorbent was imagining by scanning electron microscopy (SEM) with Vega3 Tescan model. SEM images helps to predict the microstructures of the fresh and fluoride treated materials. The qualitative detection and localization of elements present in the materials was identified by energy dispersive X-ray (EDAX-Bruker Nano GMBH, Germany) analyzer.

2.6. Statistical tools

The Microcal Origin (Version 8.0) software was used for the data computation. The regression correlation coefficient (r), standard deviation (sd) and chi-square analysis (χ^2) helps in the prediction of best fit isotherm model.

3. Results and discussion

3.1. Characterization of the sorbents

3.1.1. FTIR analysis

An FTIR spectrum is an essential tool to identify the functional groups present in the adsorbents. Figs. 1a and b represent the FTIR spectra of AA and CAA respectively. A sharp band at 1742 cm^{-1} confirms the presence of carbonyl group in both AA and CAA. In Fig. 1b, the band in the region of 3000–3600 cm^{-1} was quietly narrowed, indicates that the hydroxyl groups in AA were oxidized into carboxylic acid group (Jeon et al., 2002). In Fig. 1c, the C=O stretching vibration was disappeared at 1745 cm^{-1} in Zr-CAA and the band in the region of 3000–3600 cm^{-1} was again narrowed due to —OH stretching of carboxylic acid which indicates the H^+ ions of carboxylic acid are replaced by metal ions. A new band was also observed at around 1605–1652 cm^{-1} for Zr-CAA sorbent, indicating the presence of metal alginate bonds in Zr-CAA (Paudyal et al., 2013). In fluoride sorbed Zr-CAA, the shifting and broadening of bands at 3425 and 1652 cm^{-1} to lower frequencies (cf. Fig. 1d) owing to the electrostatic adsorption between the fluoride and the sorbent (Smith, 1998; Zhou, Zhang, & Guo, 2005). Similar reports were obtained for La-CAA and fluoride sorbed La-CAA material.

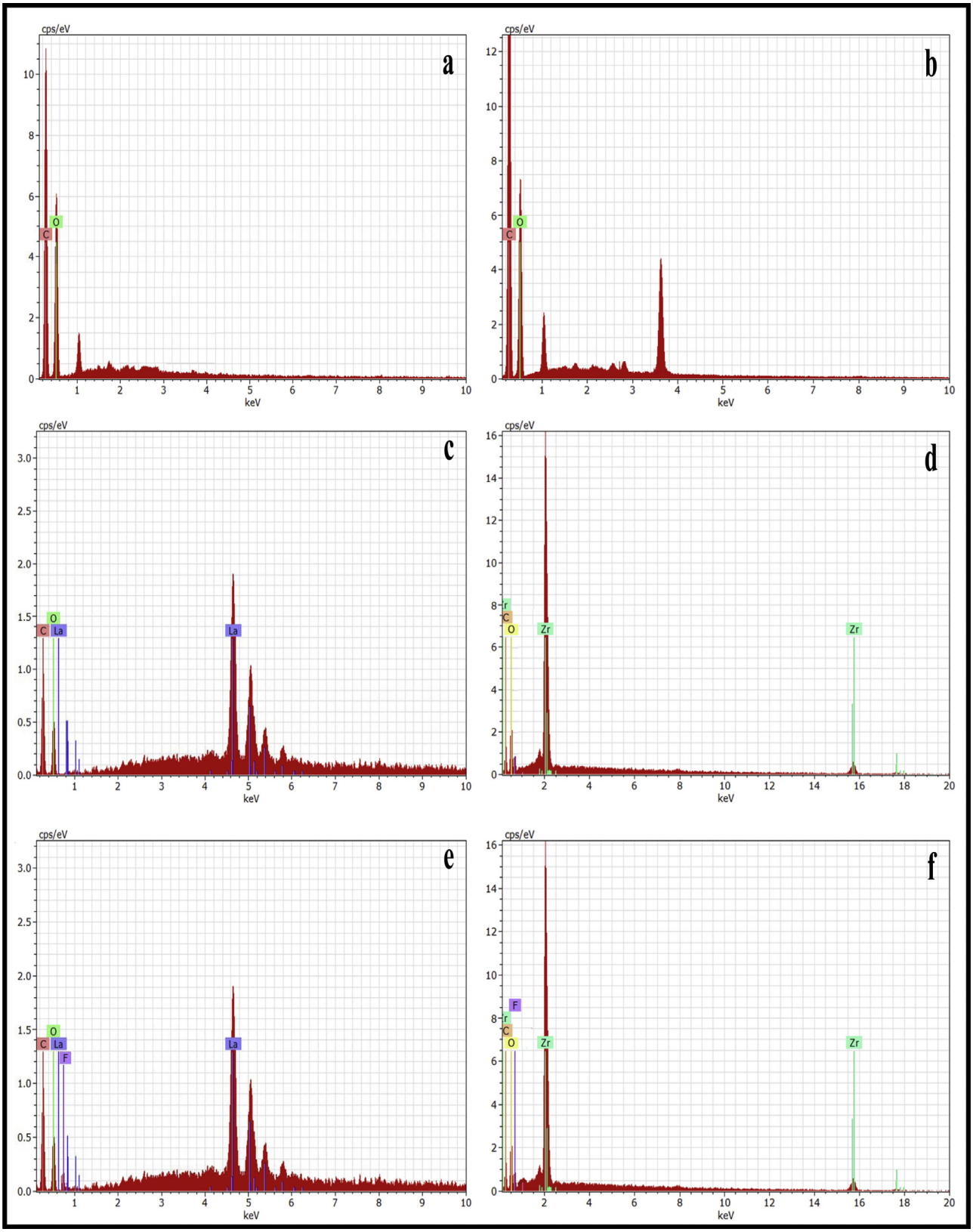

Fig. 2. EDAX spectra of (a) AA, (b) CAA, (c) La-CAA, (d) Zr-CAA, (e) fluoride sorbed La-CAA and (f) fluoride sorbed Zr-CAA.

3.1.2. SEM and EDAX analysis

The composition of elements in the biosorbents and fluoride treated biosorbents were quantitatively determined using EDAX analysis. The EDAX spectra of AA, CAA, M-CAA and fluoride sorbed M-CAA are shown in Fig. 2. The EDAX spectra of AA and CAA are shown in Fig. 2a and b respectively. The elemental peaks of C (0.24 keV), O (0.33 keV) and Na (1.06 keV) were observed in AA, but in CAA the intensity of C and O was found to be increased,

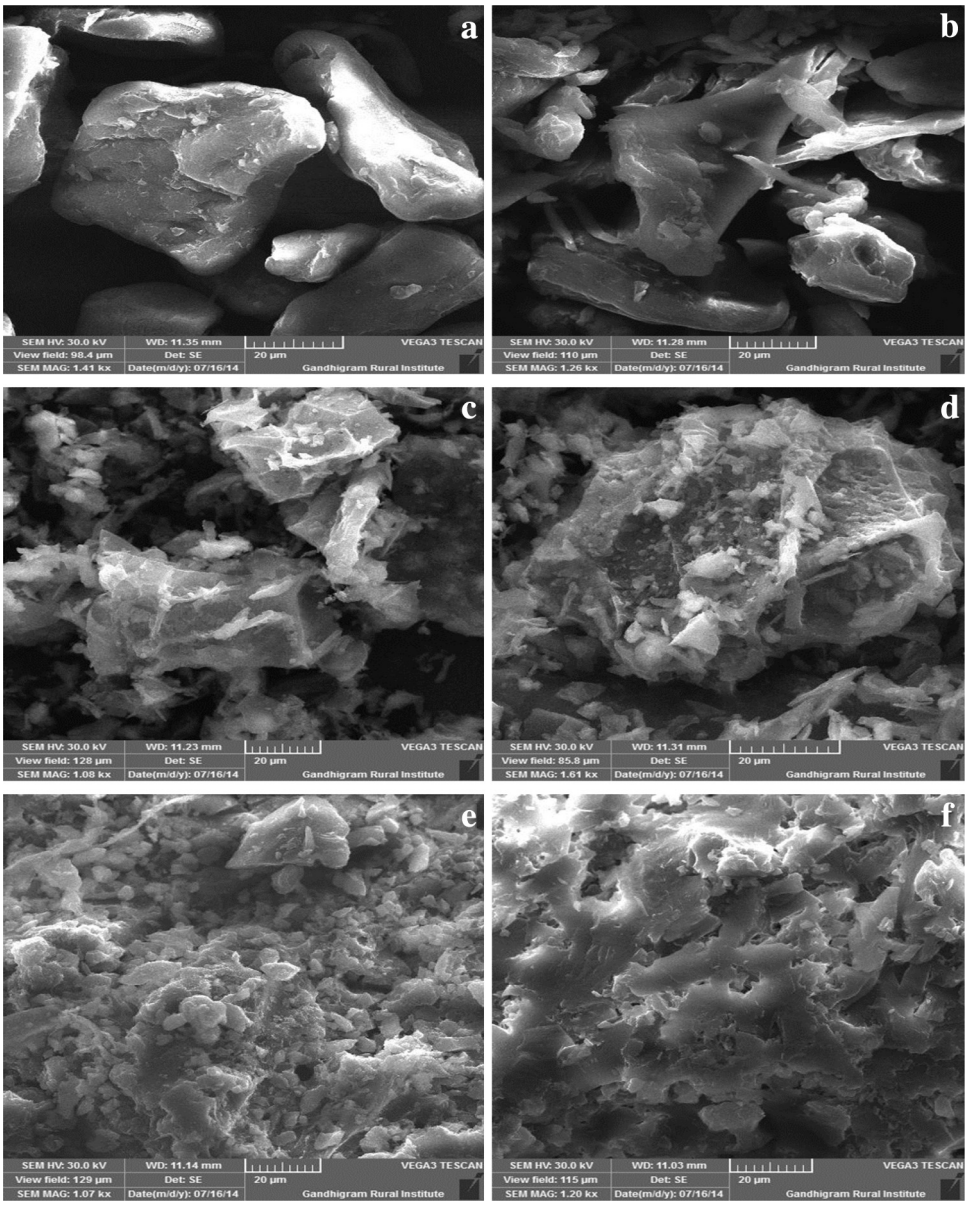

Fig. 3. SEM images of (a) AA, (b) CAA, (c) La-CAA, (d) Zr-CAA, (e) fluoride sorbed La-CAA and (f) fluoride sorbed Zr-CAA.

indicating that number of carboxylic acid groups was increased through oxidation and one more peak was observed at (3.59 keV) due to K from $KMnO_4$. The new peaks were obtained that is assigned to La at 0.66, 4.66, 5.06, 5.41, and 5.80 keV for La-CAA (cf. Fig. 2c) while new peaks were observed at 2.08 and 15.85 keV are assigned to Zr (cf. Fig. 2d), suggesting that these metal ions were effectively coordinated on CAA. The fluoride sorption was occurred on M-CAA which were confirmed by the presence of fluoride peaks in fluoride sorbed M-CAA at (0.72 keV) (cf. Fig. 2e and f). SEM images of AA, CAA, M-CAA and fluoride sorbed M-CAA are shown in Fig. 3. Fig. 3a and b visibly shows there is no metallic spots on AA and CAA. But in Fig. 3c and d, the metallic spots are spread over on M-CAA. After fluoride sorption, Fig. 3e and f surface shows glowing metallic spots that are absent, which concluded that the fluoride is sorbed on M-CAA.

3.1.3. pH_{zpc} analysis

The pH_{zpc} will display the preference for ionic species and net surface charge of the adsorbent. At pH_{zpc} value of the material possesses zero charge, below which it possess positively charged surface and above which it possess negatively charged surface. The surface morphological changes of CAA and M-CAA were also confirmed by the shifting of pH_{zpc} values. The pH_{zpc} of AA and CAA is 2.83 and 2.31 respectively (Jeon, Yoo, & Hoell, 2005) where as the La(III) and Zr(IV) loaded CAA the values were shifted to 4.09 and 4.42 respectively, which obviously indicates the occurrence of surface charge changes in M-CAA.

3.2. Optimization of contact time for maximum fluoride sorption

To find out the minimum contact time for maximum DC, the experiments were carried out by different contact time in the range of 10–60 min with 0.1 g of the sorbent and 50 mL of 10 mg/L initial fluoride solution. Fig. 4a shows that CAA was reached saturation at 50 min but M-CAA sorbents reached saturation at 30 min in a rapid manner. Among the biosorbents, La-CAA and Zr-CAA sorbents possess enhanced DC of 3137 and 4064 mgF^-/kg respectively, when compare CAA which possesses the DC of 880 mgF^-/kg. So, further

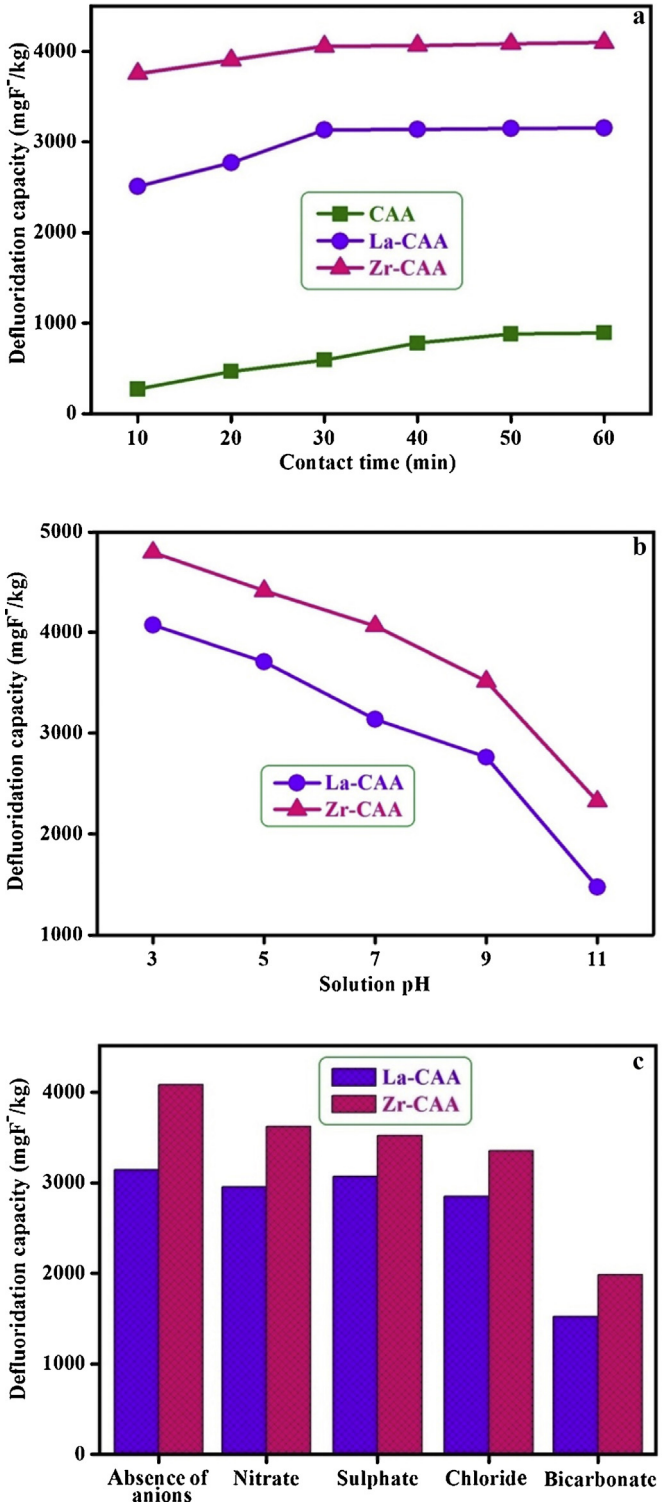

Fig. 4. (a) Influence of contact time on the DC of CAA, La-CAA and Zr-CAA. (b) Effect of pH on the DC of M-CAA. (c) Fluoride selectivity of M-CAA in the presence of co-anions.

studies are limited to M-CAA sorbents as they possess higher DC with minimum time. Hence, 30 min was chosen as period of contact time for the successive experiments of M-CAA.

3.3. Effect of solution pH

The pH of the solution is one of the most significant parameters alter the fluoride uptake capacity of the sorbent. Hence the experiments were done at five different initial pH levels viz., 3, 5, 7, 9 and 11 by maintaining all other influencing parameters as constant at room temperature. Fig. 4b shows that the DC of M-CAA sorbents were found to be influenced by solution pH. La-CAA possess a maximum DC of 4069 mgF^-/kg at pH 3 and a gradual decrease in DC with increase in pH and a minimum DC of 1475 mgF^-/kg was obtained at pH 11. The parallel results was also observed for Zr-CAA, which shows a maximum DC of 4789 at pH 3 and minimum DC of 2324 mgF^-/kg at pH 11 respectively. The main reason could be, the observed pH_{zpc} values of both La-CAA and Zr-CAA are around 4. Below pH_{zpc}, both La-CAA and Zr-CAA possess more positively charges and hence their DC was not affected even in the formation of HF. Similarly by increasing pH value (i.e., above 4) both La-CAA and Zr-CAA possess negatively charged surface and hence their DC gets decreased, i.e., there is a repulsive interaction between negatively charged fluoride and M-CAA (Zhou, Cheng, Yu & Liu 2011). In addition, the hydroxyl ions will battle with fluoride ions for occupying the active sites of the sorbent during fluoride sorption in alkaline pH ranges.

3.4. Interfering anions on fluoride removal

The normal water contains other co-anions in addition to fluoride and they will interrupt the DC of the material. Hence the DC of M-CAA in the presence of other challenging anions those are naturally present in the drinking water like Cl^-, NO_3^-, SO_4^{2-}, and HCO_3^- ions were carried out. The initial fluoride ion concentration was fixed as 10 mg/L whereas the interfering anions concentrations were fixed as 200 mg/L and all other influencing parameters as constant at room temperature. Fig. 4c shows the effect of other anions on DC of M-CAA. There is no momentous influence on M-CAA in the presence of Cl^-, NO_3^- and SO_4^{2-} ions. But, in the presence of HCO_3^- ion, the DC of M-CAA sorbents were decreased which is due to increase in solution pH and the OH^- ions reducing the active sites of the sorbents during fluoride sorption.

3.5. Sorption isotherms

Sorption isotherms are mathematical models that illustrate the delivery of the adsorbate species among solid and liquid phases, based on the hypothesis that are associated to the homogeneity or heterogeneity of the solid surface, possibility of interaction and type of coverage between the adsorbate. The sorption data of M-CAA was analyzed using four important isotherms viz., Freundlich (1906), Langmuir (1916), Dubinin–Radushkevich (Dubinin, Zaverina, & Radushkevich, 1947) and Temkin (Temkin & Pyzhev, 1940) isotherms.

The applicability of Freundlich equation was indicated by the linear plot of log q_e vs. log C_e. The obtained $1/n$, n and k_F values are presented in Table 1. The value of $1/n$ lies between 0 to 1 and n values lies between 1 and 10 represent the favorable conditions for sorption. The linear plot of C_e/q_e vs. C_e indicates the applicability of Langmuir isotherm. The calculated values of Q° and b are listed in Table 1. The R_L values lies in the range between 0 and 1 indicate the sorption process was favorable. In D-R isotherm, the values of k_{DR} and X_m were computed from the slope and intercept of the plot ln q_e vs. ε^2 and are listed in Table 1. Temkin isotherm was carried out by plotting the quantity sorbed q_e against ln C_e. The values of k_T and B_1 were determined from the slope and intercept of the linear plot q_e vs. ln C_e and are listed in Table 1. The higher r values and the lower sd values indicate the applicability of particular isotherm.

To identify the best isotherm model, non-linear χ^2 analysis has been carried out for the quantification of fluoride sorption onto M-CAA. The χ^2 values helps to find the best fit isotherm and the results are presented in Table 1. Based on the analysis, the best fit model

Table 1
Isotherm models of La-CAA and Zr-CAA on fluoride removal.

Isotherms	Parameters	La-CAA			Zr-CAA		
		303 K	313 K	323 K	303 K	313 K	323 K
Freundlich	$1/n$	0.465	0.410	0.287	0.353	0.341	0.288
	n	2.151	2.439	3.484	2.833	2.933	3.472
	$k_{F(mg/g)(L/mg)^{1/n}}$	1.758	2.042	2.679	2.999	3.177	3.631
	r	0.989	0.997	0.981	0.974	0.985	0.981
	sd	0.016	0.014	0.053	0.041	0.037	0.029
	χ^2	0.003	0.005	0.017	0.090	0.011	0.013
Langmuir	Q°(mg/g)	6.098	5.917	5.128	6.579	6.410	6.369
	b (L/g)	0.315	0.405	0.867	0.704	0.872	1.236
	R_L	0.241	0.198	0.103	0.124	0.103	0.075
	r	0.985	0.987	0.970	0.899	0.927	0.949
	sd	0.044	0.026	0.076	0.051	0.039	0.041
	χ^2	0.004	0.007	0.019	0.010	0.012	0.017
Dubinin – Radushkevich	k_{DR} (mol^2/J^2)	6.90E−7	5.09E−7	3.49E−7	2.89E−7	2.08E−7	1.19E−7
	X_m (mg/g)	4.350	4.450	4.660	5.310	5.260	5.370
	E (kJ mol^{-1})	2.997	4.189	6.591	6.190	5.042	4.404
	r	0.987	0.993	0.926	0.906	0.943	0.953
	sd	0.043	0.034	0.092	0.097	0.072	0.065
	χ^2	0.008	0.001	0.021	0.015	0.014	0.026
Temkin	k_T (L/g)	8.18E+00	1.64E+01	2.60E+02	8.84E+01	1.97E+02	5.65E+02
	B_1	1.476	1.401	1.051	1.467	1.359	1.301
	r	0.978	0.985	0.889	0.901	0.926	0.949
	sd	0.108	0.081	0.394	0.390	0.336	0.297
	χ^2	0.610	0.864	1.565	1.775	2.003	2.408

was arrived in the following order: Freundlich > Langmuir > D-R > Temkin for fluoride sorption onto M-CAA sorbents.

3.6. Thermodynamic studies

The values of thermodynamic parameters help to test the spontaneous occurrence of a given process as well as the viability of operation at given temperature. Thermodynamic parameters viz., standard free energy change (ΔG°), standard enthalpy change (ΔH°) and standard entropy change (ΔS°) were calculated by Khan and Singh method (Khan & Singh, 1987). The calculated results of thermodynamic parameters are presented in Table 2. The negative values of ΔG° and positive value of ΔH° indicates that the defluoridation was governed by spontaneous and endothermic in nature. The positive value of ΔS° indicates the fluoride removal is stable one.

3.7. Sorption kinetic models

The two main types of sorption kinetic models, namely reaction-based and diffusion-based models were adopted to fit the experimental data of M-CAA.

3.7.1. Reaction-based models

The most commonly used pseudo-first-order (Lagergren, 1898) and pseudo-second-order (Ho, 2006) models were employed to explain the solid/liquid adsorption. Plots of log $(q_e - q_t)$ against t give straight line to indicate the applicability of pseudo-first-order model. The slopes of the straight line plots of log $(q_e - q_t)$ against t sorption at different temperatures viz., 303, 313 and 323 K give the pseudo-first-order rate constant (k_{ad}) and r values of both La-CAA and Zr-CAA are listed in Tables S1 and S2, respectively. In addition, the fitness of the data and the values of q_e, k, h and r of the pseudo-second-order model were obtained from the plots of t/q_t vs. t for fluoride sorption at different temperatures viz., 303, 313 and 323 K of both La-CAA and Zr-CAA are presented in Tables S1 and S2 (see in supplementary data), respectively. The correlation coefficient (r) values observed for the pseudo-second-order model are higher than the pseudo-first-order model indicating the applicability of the pseudo-second-order model.

Table 2
Thermodynamic parameters of La-CAA and Zr-CAA on fluoride sorption.

Thermodynamic parameters		La-CAA	Zr-CAA
ΔG° (kJ mol^{-1})	303 K	−5.01	−3.54
	313 K	−4.79	−3.33
	323 K	−4.30	−2.77
ΔH° (kJ mol^{-1})		15.75	15.26
ΔS° (kJ mol^{-1} K^{-1})		0.04	0.04

3.7.2. Diffusion-based models

For a solid–liquid sorption process, the solute transfer is usually characterized either by particle diffusion or intraparticle diffusion control. Both particle (Chanda, O'Driscoll, & Rempel, 1983) and intraparticle (Weber & Morris, 1964) diffusion models were used to describe the fluoride removal by M-CAA. The respective straight line plots of ln $(1 - C_t/C_e)$ vs. t and q_t vs. $t^{0.5}$ indicates the applicability of both particle and intraparticle diffusion models. The k_p, k_i and r values at different temperatures viz., 303, 313 and 323 K for both particle and intraparticle diffusion models of La-CAA and Zr-CAA are given in Tables S1 and S2 (see in supplementary data), respectively. The higher r values obtained for both particle and intraparticle diffusion models suggest that the fluoride diffusion on M-CAA follows both the models.

3.8. Feasible fluoride removal mechanism of M-CAA

The feasible fluoride removal mechanism of M-CAA was given in Fig. 5. CAA has appreciable fluoride removal capacity and it removes fluoride via adsorption. But in M-CAA, metal ions formed coordination with CAA and also get exchanged for H^+ ions of the carboxyl groups, which contains oxygen atom as an electron pair donor to the metal ions (Lewis acid).

M-CAA removes fluoride by means of electrostatic adsorption. In addition, the neutralization of metal ions in does not take

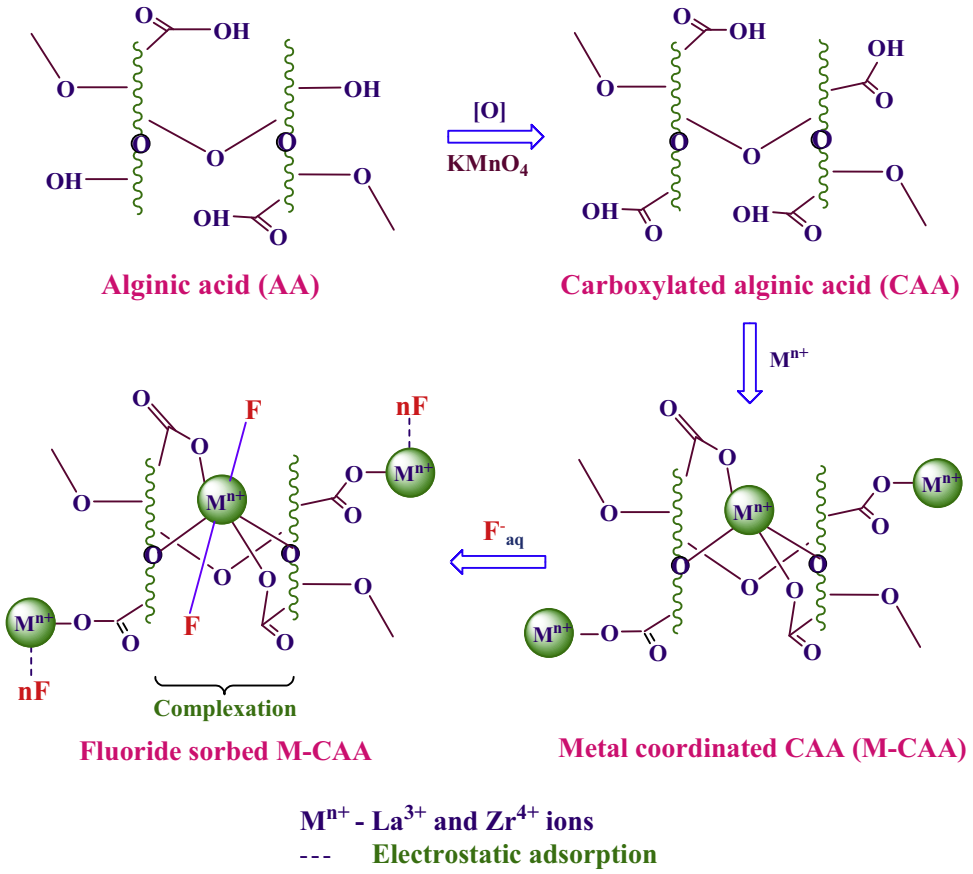

Fig. 5. Feasible fluoride removal mechanism of M-CAA.

place which, in turn permits entrapping of fluoride from the solution due to the complexation mechanism (Dabrowski, Hubicki, Podkoscielny, & Robens, 2004). In general, M-CAA possess higher DC than CAA, because M-CAA removes fluoride by both adsorption and complexation, where as CAA removes fluoride by adsorption only. Among M-CAA, Zr-CAA possessed higher DC than La-CAA. The reason is Zr-CAA possess higher valence Zr^{4+} ions which enhances its selectivity towards fluoride than La-CAA which possess La^{3+} ions.

3.9. Application of M-CAA at field conditions

The suitability of M-CAA was also tested with a field sample taken from a nearby fluoride widespread village. About 50 mL of fluoride water sample and 0.1 g of sorbent was shaken with constant time at room temperature. The field trial results are presented in Table 3. M-CAA sorbents reduced the fluoride concentration below the tolerance limit in the field fluoride water. Eventhough the concentration of other anions are higher than fluoride concentration in field water, both La-CAA and Zr-CAA removes fluoride selectively. In addition to fluoride, the level of other water quality parameters was also reduced. Hence, M-CAA sorbents can be effectively employed for removing the fluoride from water.

Table 3
Application of La-CAA and Zr-CAA at field conditions.

Water quality parameters	Before treatment	After treatment	
		La-CAA	Zr-CAA
F^- (mg/L)	3.01	0.90	0.85
pH	8.37	7.89	7.65
Cl^- (mg/L)	306	276	263
SO_4^{2-} (mg/L)	535	511	499
NO_3^- (mg/L)	68	53	38
HCO_3^- (mg/L)	203	164	147
Total hardness (mg/L)	424	401	374
Total dissolved solids (mg/L)	1078	979	936

4. Conclusions

The synthesized CAA and M-CAA was characterized using FTIR, SEM with EDAX analysis. The developed M-CAA possesses higher DC than CAA. Among M-CAA, Zr-CAA show higher DC than La-CAA. The DC of M-CAA sorbents were influenced by solution pH and slightly by the bicarbonate ions. The sorption of fluoride onto M-CAA follows Freundlich isotherm. The nature of fluoride removal was spontaneous and endothermic. The kinetics of the reaction followed pseudo-second-order model and intraparticle diffusion pattern. The defluoridation mechanism was governed by electrostatic adsorption and complexation. The field trial results of M-CAA materials showed that could be effectively utilized for defluoridation. The developed M-CAA materials are low cost, eco-friendly, biodegradable and biocompatible sorbents for selective fluoride removal.

Acknowledgement

The authors are thankful to Department of Science and Technology – Science and Engineering Research Board (No. SR/FT/CS-43/2011 dt. 24-05-2012), New Delhi, India for the provision of financial support to carry out this research study.

References

APHA. (2005). *Standard methods for the examination of water and waste water*. Washington, DC: American Public Health Association.

Chanda, M., O'Driscoll, K. F., & Rempel, G. M. (1983). Sorption of phenolics onto cross-linked poly(4-vinyl pyridine). *Reactive Polymers*, *1*, 281–293.

Dabrowski, A., Hubicki, Z., Podkoscielny, P., & Robens, E. (2004). Selective removal of the heavy metal ions from waters and industrial wastewaters by ion-exchange method. *Chemosphere*, *56*, 91–106.

Dubinin, M. M., Zaverina, E. D., & Radushkevich, L. V. (1947). Sorption and structure of active carbons. *Journal of Physical Chemistry*, *21*, 1351–1362.

Freundlich, H. M. F. (1906). Uber die adsorption in losungen. *International Journal of Research in Physical Chemistry and Chemical Physics*, *57A*, 385–470.

Googerdchian, F., Moheb, A., & Emadi, R. (2012). Lead sorption properties of nanohydroxyapatite–alginate composite adsorbents. *Chemical Engineering Journal*, *200–202*, 471–479.

Ho, Y. S. (2006). Second-order kinetic model for the sorption of cadmium onto tree fern: A comparison of linear and non-linear methods. *Water Research*, *40*, 119–125.

Jayakumar, R., Rajkumar, M., Freitas, H., Selvamurugan, N., Nair, S. V., Furuike, T., et al. (2009). Preparation, characterization, bioactive and metal uptake studies of alginate/phosphorylated chitin blends films. *International Journal of Biological Macromolecules*, *44*, 107–111.

Jeon, C., Park, J. Y., & Yoo, Y. J. (2002). Characteristics of metal removal using carboxylated alginic acid. *Water Research*, *36*, 1814–1824.

Jeon, C., Yoo, Y. J., & Hoell, W. H. (2005). Environmental effects and desorption characteristics on heavy metal removal using carboxylated alginic acid. *Bioresource Technology*, *96*, 15–19.

Zhou, J., Cheng, Y., Yu, J., & Liu, G. (2011). Hierarchically porous calcined lithium/aluminum layered double hydroxides: Facile synthesis and enhanced adsorption towards fluoride in water. *Journal of Material Chemistry*, *21*, 19353–19361.

Khan, A. A., & Singh, R. P. (1987). Adsorption thermodynamics of carbofuran on Sn(IV) arsenosilicate in H^+ Na^+ and Ca^{2+} forms. *Colloids and Surfaces*, *24*, 33–42.

Lagergren, S. (1898). Zur theorie der sogenannten adsorption gelöster stoffe. *Kungliga Svenska Vetenskapsakademiens*, *24*, 1–39.

Langmuir, I. (1916). The constitution and fundamental properties of solids and liquids. *Journal of American Chemical Society*, *38*, 2221–2295.

Lopez-Ramon, M. V., Stoeckli, F., Moreno-Castilla, C., & Carrasco-Marin, F. (1999). On the characterization of acidic and basic surface sites on carbons by various techniques. *Carbon*, *37*, 1215–1221.

Lu, N. C., & Liu, J. C. (2010). Removal of phosphate and fluoride from wastewater by a hybrid precipitation-microfiltration process. *Separation and Purification Technology*, *74*, 329–335.

Meenakshi, S., & Viswanathan, N. (2007). Identification of selective ion-exchange resin for fluoride sorption. *Journal of Colloid and Interface Science*, *308*, 438–450.

Ndiaye, P. I., Moulin, P., Dominguez, L., Millet, J. C., & Charbit, F. (2005). Removal of fluoride from electronic industrial effluent by RO membrane separation. *Desalination*, *173*, 25–32.

Pandi, K., & Viswanathan, N. (2014). Synthesis of alginate bioencapsulated nanohydroxyapatite composite for selective fluoride sorption. *Carbohydrate Polymers*, *112*, 662–667.

Paudyal, H., Pangeni, B., Inoue, K., Kawakita, H., Ohto, K., Ghimire, K. N., et al. (2013). Preparation of novel alginate based anion exchanger from Ulva japonica and its application for the removal of trace concentrations of fluoride from water. *Bioresource Technology*, *148*, 221–227.

Sairam Sundaram, C., Viswanathan, N., & Meenakshi, S. (2009). Fluoride sorption by nano-hydroxyapatite/chitin composite. *Journal of Hazardous Materials*, *172*, 147–151.

Smith, B. (1998). *Infrared spectral interpretation-a systematic approach*. London: CRC Press.

Tahaikt, M., El Habbani, R., Ait Haddou, A., Achary, I., Amor, Z., Taky, M., et al. (2007). Fluoride removal from groundwater by nanofiltration. *Desalination*, *212*, 46–53.

Temkin, M. J., & Pyzhev, V. (1940). Recent modifications to Langmuir isotherms. *Acta Physiochim URSS*, *12*, 217–222.

Varma, A. J., Deshpande, S. V., & Kennedy, J. F. (2004). Metal complexation by chitosan and its derivatives: A review. *Carbohydrate Polymers*, *55*, 77–93.

Vasudevan, S., Lakshmi, J., & Sozhan, G. (2009). Studies on Mg-Al-Zn alloy as an anode for the removal of fluoride from drinking water in an electrocoagulation process. *Clean*, *37*, 372–378.

Viswanathan, N., & Meenakshi, S. (2008). Enhanced fluoride sorption using La(III) incorporated carboxylated chitosan beads. *Journal of Colloid and Interface Science*, *322*, 375–383.

Viswanathan, N., & Meenakshi, S. (2009a). Synthesis of Zr(IV) entrapped chitosan polymeric matrix for selective fluoride sorption. *Colloids and Surfaces B: Biointerfaces*, *72*, 88–93.

Viswanathan, N., & Meenakshi, S. (2009b). Enhanced and selective fluoride sorption on Ce(III) encapsulated chitosan polymeric matrix. *Journal of Applied Polymer Science*, *112*, 1114–1121.

Viswanathan, N., & Meenakshi, S. (2010). Enriched fluoride sorption using alumina/chitosan composite. *Journal of Hazardous Materials*, *178*, 226–232.

Weber, W. J., & Morris, J. C. (1964). Equilibria and capacities for adsorption on carbon. *Journal of the Sanitary Engineering Division*, *90*, 79–91.

WHO. (2006). *Guidelines for drinking-water quality* (First Addendum to Third Edition). Available from: http://www.who.int/water_sanitation_health/dwq/gdwq0506.pdf

Yu, X., Tong, S., Ge, M., & Zuo, J. (2013). Removal of fluoride from drinking water by cellulose@hydroxyapatite nanocomposites. *Carbohydrate Polymers*, *92*, 269–275.

Zhou, D., Zhang, L., & Guo, S. (2005). Mechanisms of lead biosorption on cellulose/chitin beads. *Water Research*, *39*, 3755–3762.